Left Coronary Artery Imaging at 7T: Initial Results using Multiple B1+ Shimming Algorithms and Targets

G. J. Metzger[1], L. Delabarre[1], X. Bi[2], S. Shah[2], S. Zuehlsdorff[2], T. Vaughan[1], K. Ugurbil[1], and P-F. van de Moortele[1]
[1]Center for Magnetic Resonance Research, University of Minnesota, Minneapolis, MN, United States, [2]Siemens Healthcare, Cardiovascular MR R&D, Chicago, IL, United States

INTRODUCTION: Performing right coronary artery imaging at 7T has been shown to improve the signal to noise (SNR) and contrast to noise (CNR) compared to 3T when using a turbo-FLASH (TFL) acquisition with an adiabatic spectrally selective RF pre-pulse (SPAIR) for lipid suppression (1). However, to date, imaging of the left coronary artery (LCA) has not been shown, with the suggested challenge being that poor myocardial-blood contrast would diminish the ability to visualize the vessels (1). The apparent lack of contrast most likely originates from the absence of sufficient transmit B1 (B1+) in the heart especially over the course of the left coronary artery which is deeper within the body than the right. In general, the contrast between the blood pool and myocardium has been shown to be similar or even greater at higher field strengths (2). To address the challenge of low peak B1+ and the known challenge of B1+ inhomogeneity at 7T in the context of imaging the LCA, multiple optimized B1+ shimming solutions within a single acquisition sequence were employed using a multi-channel surface array coil. This strategy allowed the LCA to be imaged at 7T with similar contrast to that achieved in the RCA but with lower SNR due to the increased distance of the former from the RF coil. To our knowledge, this is the first demonstration of left coronary artery imaging at 7T.

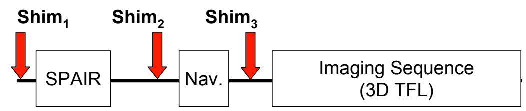

Figure 1: Angiography sequence with RF shim triggers.

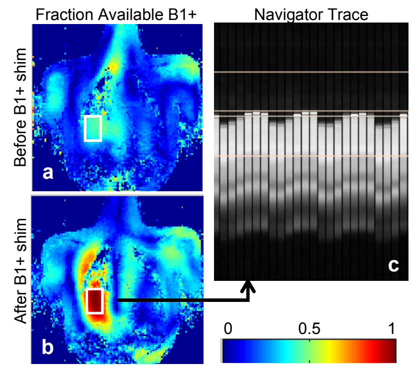

Figure 2: Fraction available B1+ before (a) and after (b) B1+ shimming in an ROI on the liver. (c) Navigator signal with gating window.

METHODS: Studies were performed on a Siemens 7T with a 16-channel transceiver TEM stripline array driven by 16, 1 kW amplifiers with independent phase and gain control (CPC, Hauppauge, NY) (3-5). Power monitoring on each channel was accomplished using a homebuilt system (6). Healthy subjects were imaged under and IRB approved protocol. For imaging, a TFL was used with an adiabatic spectrally selective RF pre-pulse (SPAIR) for T1 lipid nulling. A vector cardiogram (VCG) was used for recording the cardiac signal and for triggering. Respiratory motion was addressed through the use of a navigator placed in the traditional position, at the lung-diaphragm interface. The navigator was used for sequence gating and slice following with a ±2.5 mm acceptance window. Other sequence parameters included: 420 FOV, 512x512 matrix, 40 slices, TR/TE 4.3/1.94 ms, 360 ms TI, 0.8x0.8x2.0 mm^3 acquired and 0.8x0.8x1.0 mm^3 reconstructed. The acquisition time was 590 ± 186 s and the average heart rates were 63±5 beats per minute. The final angiography volume was positioned using 3 point planning on a low resolution dataset to best cover the LCA. Localized B0 shimming was performed on volumetric single breath-hold phase maps (12).

In order to perform subject dependent B1+ shimming, complex B1+ maps were estimated for each of the 16 channels using fast, low flip angle, multi channel B1+ calibration scans (7), each within a single breath hold (8) and with cardiac triggering. A first B1+ calibration scan in a coronal plane crossing the liver apex was used to minimize destructive interferences within a ROI (see Fig. 2) positioned at the level of the navigator ($Shim_2$). A second B1+ calibration scan in the plane of the angiography volume was used to optimize: i) the inversion pulse for transmit efficiency ($Shim_1$) and ii) the excitation pulse for a tradeoff between efficiency and homogeneity ($Shim_3$). The tradeoff solution was accomplished by constraining our B1+ efficiency optimization algorithm with an upper limit on B1+ inhomogeneity defined as the (mean/std) ratio of |B1+|. Both $Shim_1$ and $Shim_3$ were optimized over the same ROI which was manually drawn over half of the heart in the imaging plane which included the LCA. Each B1+ shim solution consisted of a table of phases and gains which could be loaded onto the amplifier's controller within ~5 µs. In order to accurately switch from one shim solution to the next, the acquisition sequence was programmed to send TTL triggers to the RF amplifier, each of which initiates the loading of the appropriate table (Fig. 1).

Even though the LCA was targeted, significant portions of the RCA could also be visualized. This allowed some preliminary comparative measurements to be made between the two vessels including contrast-to-noise (CNR), signal-to-noise (SNR). Vessel length was measured for the LCA and sharpness and diameter for the LAD using similar analysis strategies as those presented previously (9,10). Curved reformatting was used to visualize the left and right coronary vessels in the imaging volume (11).

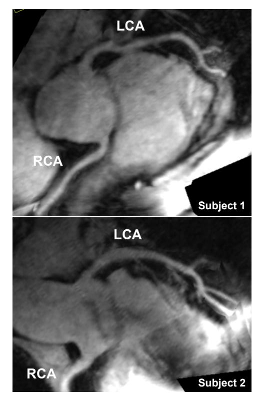

Figure 3: Curved reformatted images from two subjects.

RESULTS: The increase in transmit efficiency at the location of the navigator in the diaphragm can be appreciated by the coronal fraction available B1+ maps (|ΣB1+| / Σ|B1+|, summation is over all 16 complex B1+ profiles) before and after implementation of $Shim_2$ (Fig. 2a and 2b). Fig. 2c shows the navigator signal with a sharp liver/lung interface with $Shim_2$ necessary for accurate slice following and gating. Navigator efficiency, which is the percent of acquisitions in the acceptance window, was 40 ± 5% for the three subjects in this comparison. A quantitative comparison of CNR and SNR between the LCA and RCA can be found in Table 1. LCA vessel lengths were 8.0 ± 0.3 and LAD sharpness and diameters were 1.6 ± 0.1, and 3.5 ± 0.7 respectively. Curved reformats of two subjects are shown in Fig. 3.

	LCA	RCA
CNR	49.5 ± 33.0	75.3 ± 46.5
SNR	61.5 ± 33.1	91.5 ± 50.0

Table 1: LCA and RCA comparison.

DISCUSSION: By using a multi-element transmit array and dynamic B1+ shimming, the LCA could be visualized with high contrast at 7T. A multi-element transceiver array and the use of multiple B1 shimming solutions for different spatial targets and/or different RF pulses in the sequence allowed RF pulses to be optimized to best suit their function and their spatial coverage given the limitations in peak B1+ and challenges of B1+ homogeneity at 7T. The origins of the RCA and LCA were on average 5.2 and 7.4 cm respectively from the chest wall. More distally the RCA tends to move closer to the chest wall or closer to anteriorly placed coils while the LCA tends to remains closer to the center of the body until the most distal sections. The challenge of achieving a relatively high B1+ for inversion in the center of the body, even when using a 16 channel transmit array surrounding the torso, necessitated the use of more efficient B1+ shim solutions. This type of solution suits the adiabatic inversion pulse because of its insensitivity to B1+ inhomogeneity. With respect to the excitation pulse, a homogeneous solution might appear to be the best at first. However, a homogeneous solution comes at a tremendous cost in efficiency and would result in unacceptably high power deposition. Therefore, a tradeoff solution was used between B1 homogeneity and efficiency.

The SNR and CNR in the RCA were slightly lower than those previously presented by others (1). Our results in the RCA could most likely be improved by including this vessel in the target ROIs used for B1+ shimming. Furthermore, both the RCA and LCA would benefit from the addition of anterior regional saturation (RSAT) bands. When RSAT pulses are used, they will benefit from an additional specific B1+ shim solution targeting the anterior chest wall and skin.

REFERENCES: [1] van Elderen, Radiology;257(1):254-259. [2] Suttie, ISMRM 2010;#3596. [3] Snyder, Magn Reson Med 2009;61(3):517-524., [4] Vaughan, USA patent 6,633,161. 2003. [5] Vaughan, USA patent 6,633,161. 2005. [6] Metzger, Magn Reson Med, In Press, PMID: 20740657 [7] Van de Moortelle, ISMRM 2009; #367. [8] Metzger, ISMRM 2010;18:#403. [9] Li, Radiology 2001;219(1):270-277. [10] Bi, J Cardiovasc Magn Reson 2006;8(5):703-707. [11] Aharon, ISMRM 2006, #365. [12] Shah. Proc ISMRM, 2009:4202.

ACKNOWLEDGEMENTS: Funding Provided by BTRC P41 RR008079, R01 EB006835, R01 EB00895 and the Keck Foundation S10 RR026783. We would also like to acknowledge Jens Guehring and colleagues for providing the Coronaviz software (Siemens, Germany) used for curved reformatting.